NANO LETTERS

Letter

pubs.acs.org/NanoLett

# Prelithiation Activates $Li(Ni_{0.5}Mn_{0.3}Co_{0.2})O_2$ for High Capacity and Excellent Cycling Stability

Zhongzhen Wu,[†] Shunping Ji,[†] Jiaxin Zheng,[†] Zongxiang Hu,[†] Shu Xiao,[†] Yi Wei,[†] Zengqing Zhuo,[†,‡] Yuan Lin,[†] Wanli Yang,[‡] Kang Xu,[§] Khalil Amine,[†,∥] and Feng Pan*,[†]

[†]School of Advanced Materials, Peking University Shenzhen Graduate School, Shenzhen 518055, China

[‡]Advanced Light Source, Lawrence Berkeley National Laboratory, Berkeley, California 94720, United States

[§]U.S. Army Research Laboratory, Adelphi, Maryland20783, United States

[∥]Electrochemical Technology Program, Chemical Sciences and Engineering Division, Argonne National Laboratory, Argonne, Illinois 60439, United States

Supporting Information

**ABSTRACT:** Transition metal oxide materials $Li(Ni_xMn_yCo_z)O_2$ (NMC) based on layered structures are expected to replace $LiFePO_4$ in automotive Li-ion batteries because of their higher specific capacity and operating potential. However, the actual usable capacity is much lower than the promised theoretical value [Uchaker, E.; Cao, G. *Nano Today* **2014** *9*, 499−524; Tarascon, J.-M.; Armand, M. *Nature* **2001** *414*, 359−367], in addition to the often poor cycling performance and the first-cycle Coulombic efficiency, for which Mn(II)-dissolution, its immobilization in solid electrolyte interface (SEI), oxidation of electrolytes by Ni, and other parasitic process thereat have been held responsible [Zhan, C., et al. *Nat. Commun.* **2013** *4*, 2437; Wang, L.,et al. *J. Solid State Electrochem.* **2009** *13*, 1157−1164; Lin, F., et al. *Nat. Commun.* **2014** *5*, 4529]. Previously, we reported a composite $Li(Ni_{0.5}Mn_{0.3}Co_{0.2})O_2$ (NMC532) depolarized by the embedded carbon nanotube (CNT) and achieved capacity close to the theoretical limit [Wu, Z., et al. *Nano. Lett.* **2014** *14*, 4700−4706]; unfortunately, this high capacity failed to be maintained in long-term cycling due to the degrading contacts between the active ingredient and CNT network. On the basis of that NMC532/CNT composite, the present work proposes a unique "prelithiation process", which brought the cathode to low potentials before regular cycling and led to an interphase that is normally formed only on anode surfaces. The complete coverage of cathode surface by this ∼40 nm thick interphase effectively prevented Mn(II) dissolution and minimized the side reactions of Ni, Co, and Mn at the NMC interface during the subsequent cycling process. More importantly, such a "prelithiation" process activated a structure containing two Li layers near the surface of NMC532 particles, as verified by XRD and first principle calculation. Hence, a new cathode material of both high capacity with depolarized structure and excellent cycling performance was generated. This new structure can be incorporated in essentially all the NMC-based layered cathode materials, providing us with an effective tool to tailor-design future new cathode materials for lithium batteries.

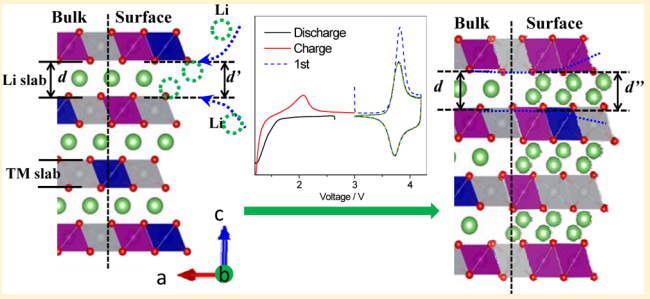


**KEYWORDS:** *prelithiation, two-layer Li, $Li(Ni_{0.5}Mn_{0.3}Co_{0.2})O_2$, carbon nanotube (CNT), solid electrolyte interface (SEI)*

Pioneering studies on intercalation chemistries enabled the birth of lithium-ion batteries, which have been the main power source for portable electronics applications. However, a limited cycle life and moderate rate capability as well as high-cost Co-rich electrode materials still restrict the market penetration of lithium-ion batteries in vehicular electrification and grid-storage applications. $LiFePO_4$ has offered relief to both cost and rate capability, but its ultimate energy density of 160 Wh/kg makes it a reluctant choice for energy-dense applications such as electric vehicles (EV) and plugged-in hybrid electric vehicles (PHEV). On the other hand, layered transition-metal oxides ($Li(Ni_xMn_yCo_z)O_2$ or NMC) materials with both higher voltage and higher capacity are expected to replace both $LiCoO_2$ and $LiFePO_4$ as the cathode of choice in the near future. However, despite the promised theoretical value (∼280 mAh/g), the capacity that can be practically accessed (∼170 mAh/g) is much lower.[1,2] The capacity decay in the long term cycling has been attributed to sustained Mn(II)-dissolution from Mn-containing cathode materials into the electrolyte and the subsequent immobilization into anode interphase,[3] accompanied by phase-transformation of NMC structure near the surface from layered to spinel, especially when charging/discharging were conducted at the high voltage (>4.2 V), high current density, or high temperatures.[4]

**Received:** June 7, 2015
**Revised:** July 2, 2015





DOI: 10.1021/acs.nanolett.5b02246
*Nano Lett.* XXXX, XXX, XXX−XXX

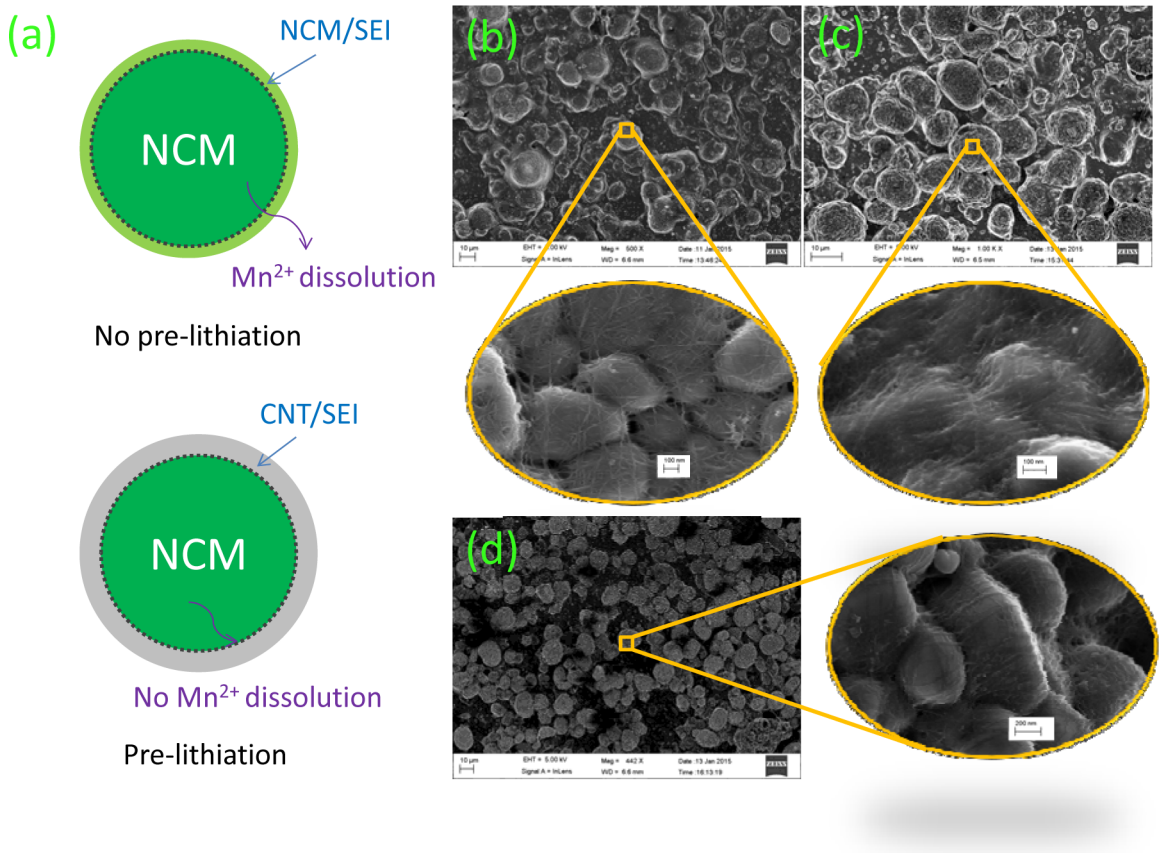


**Figure 1.** Schematic illustration of SEI generated by prelithiation and SEM of the prepared samples: (a) The solid electrolyte interphase engineered by the prelithiation protocol increases the de facto Coulombic efficiency and maintains high reversible capacity by preventing Mn(II)-dissolution; (b) SEM images of the as-prepared NMC532/CNT sample, (c) sample prelithiated to 1.2 V and (d) sample directly charged to 4.2 V. The insets in (b, c, d) magnified the corresponded areas as marked by yellow squares.

Furthermore, the transition metal elements Ni, Co, or Mn in bulk NMC will also experience an irreversible loss due to the side reaction with electrolyte, from which part of the products form surface deposition in the first charging process, and leads to high surface impedance, low Coulombic efficiency, and low capacity utilization.[5]

In our previous work we designed a composite cathode based on $Li(Ni_{0.5}Mn_{0.3}\ Co_{0.2})O_2$ (NMC532), which was effectively depolarized by the carbon nanotubes (CNT) embedded therein, and achieved capacity (about 250 mAh/g) close to the theoretic value as calculated by the first principle method when cycling between 3.0 and 4.8 V with the high voltage electrolyte.[6] But in that composite, the entanglement between the CNT network and the active NMC532 particles was insufficient to maintain the achieved high capacity during long-term cycling. Moreover, the exposure of NMC532 particles to electrolytes still led to sustained Mn(II)-dissolution and subsequent side reactions. In fact, numerous efforts have been made to insulate NMC particles from electrolyte on the purpose to mitigate these parasitic reactions, a typical of which is coatings of $Al_2O_3$, ZnO, or $TiO_2$ on the NMC particles by atomic layer deposition (ALD).[7−9] Nevertheless, due to the low ion and electron conductivity of those oxides, the coating thickness has to be carefully restricted within nanometers (nm), and the improvements brought by the coating are limited. More recently, solid electrolyte materials such as LiPON, $Li_2TiO_3$, and $LiTaO_3$ were also applied as thin coatings, which, because of their electrolyte nature, incurred further compromise to the electronic conductivity.[10−12] Needless to say, an ideal coating should render the interface with a certain thickness for effective protection as well as excellent conductivities for both ion and electron.

Here, we report a novel in situ coating process to protect NMC particles by leveraging the interphasial chemistry knowledge. The cathode was hence "pre-lithiated" to low potential before normal cycling between 3.0−4.5 V started. Such prelithiation would induce reduction of electrolyte and formed an SEI that is normally found only on anode surfaces. A thus-formed SEI covered both NMC532 particle and the embedded CNT network with a 40 nm thickness, providing a well-wired nanocomposite having both high ion (from SEI) and electronic conductivities (from CNT). Additionally, since this electronic-insulating interphase physically segregated NMC particles from electrolyte exposure, Mn(II)-dissolution, and all the undesired side reactions were prevented. Cathode materials based on such prelithiated NMC532 demonstrated not only excellent cycling performance due to the protective interphase, but also a high capacity of 185 mAh/g at 4.2 V provided by a unique two-layer Li structure that was created by the "prelithiation" process as revealed by detailed structural characterization and computations.

The NMC532 particles and the NMC532/CNT composite materials in this work were prepared by the coprecipitation and vacuum filtration method as described in the previous work,[6] as



DOI: 10.1021/acs.nanolett.5b02246
Nano Lett. XXXX, XXX, XXX−XXX

shown in Supporting Information Figure S1. The NMC532 particles consisted of 5−10 $\mu$m spherical secondary particles aggregated into submicron-sized primary particles with a narrow distribution in the range of 300−500 nm. The free-standing, binder-free NMC532/CNT composite cathode was achieved, and the CNT and the NMC532 particles were mixed at a ratio of 5:95. After assembled in the cell, the batteries were prelithiated to 1.8, 1.5, 1.2, and 0.5 V, respectively, before the conventional cyclings between 3.0 and 4.2 V started. A pristine NMC that was directly charged to 4.2 V without being prelithiated and a sample of NMC532 prepared by the conventional slurry coating method were also included as references for comparison.

A schematic illustration of how prelithiation affects the surface morphology of NMC particles is shown in Figure 1a, and SEM images of various NMC532/CNT cathodes experiencing varying charging protocols are shown in Figure 1b,c,d. The as-prepared sample obviously consists of NMC532 secondary particles constructed upon the 300−500 nm primary particles as building blocks which are intimately buried under the 3D CNT network and homogeneously distributed. From the inset it seems that such connection is loose, as characterized by the "voids" between the two components. However, a gelatinous coating was deposited on the surface of NMC532 particles once prelithiation to 1.2 V was applied, which tightly compressed NMC532 and CNT together as shown in the inset of Figure 1c. Such an intimate contact between the electron-conduction channel CNT and active NMC532 particles is also seen on the sample directly charged to 4.2 V, but it seems that the novel SEI formed during the prelithiation is apparently thicker on CNT than on NMC particles. Very likely the electrolyte reduction is first induced on CNT, burying this electronically conductive channel with ionic conductive coating. A significant decrease in the overall impedance is recorded with the prelithiated sample by EIS, as compared with the sample without prelithiation and the slurry sample, as shown in Figure S2.

The surface compositions of the three samples are investigated by XPS, as shown in Figure S3a, and the data are summarized in the table of Figure S3b. Compared with the pristine sample composed of mainly elemental C, the proportions of Li, O, F, Ni, Co, and Mn increased when charged to 4.2 V, which arose as the consequence of electrolyte/cathode reactions that consume both Li source as well as transition metal ingredients from the active particles. However, in the sample prelithiated to 1.2 V, surface species containing only Li, O, and F appear, with almost none of Ni, Co, and Mn being detected. This discrepancy in interphasial chemical composition clear indicates that prelithiation might have excluded the transition metals from participating the irreversible interphasial reactions, and the original stoichiometry of NMC particle could be maintained near the surface region.

To reveal the interphase thickness formed on the composite as well as its depth-profile of chemical compositions, $Ar^+$-sputtering was conducted on the samples by XPS, and the data were collected at each 10 nm interval from the surface. The signals corresponding to Ni, Mn, and Co at varying depths from the surface into the bulk of the NMC532 particles are shown in Figure 2 and Figure S4. The Ni 2p spectra of as-prepared samples are characterized by two main lines Ni $2p_{3/2}$ and Ni $2p_{1/2}$, accompanied by two intensive shakeup satellites S1 and S2 typical of $Ni^{2+}$ ions.[13] However, a noticeable shift in

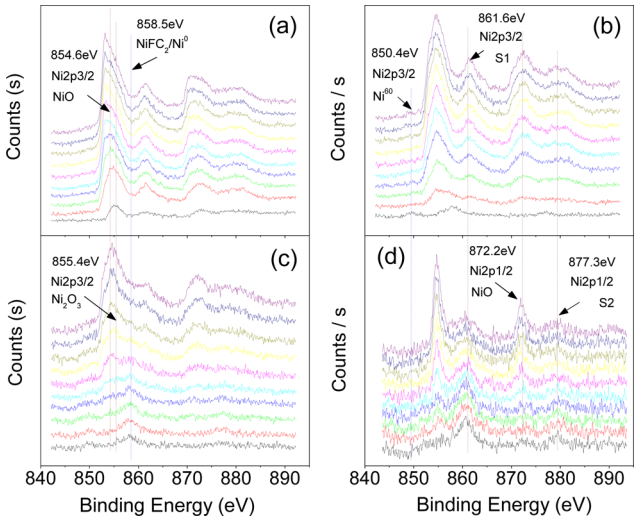


**Figure 2.** Depth profiles of Ni element in various NMC532/CNT composite cathodes: (a) As-prepared sample, (b) sample directly charged to 4.2 V, (c) sample prelithiated to 1.2 V, and (d) sample recharged to 4.2 V after prelithiation. The data were collected at a 10 nm interval from surface to the core of the NMC532 particles.

the maximum of Ni $2p_{3/2}$ line to lower binding energy was observed with increasing etching depth. The value of binding energy close to that of $LiNiO_2$ was detected and attributed to $Ni^{3+}$ ions based on the simple ionic model.[14,15] For the spectral of the other two samples, new peaks with the binding energy of 858.5 and 850.4 eV appear near the surface of the cathode. The former was observed previously and was believed to relate to a $Ni^{2+}$ containing species produced by the reaction with electrolyte,[16,17] while the latter corresponds to metallic nickel.[18] The shift of these peaks reveal the transition from interphasial to bulk region, providing an quantitative measurement for the formed interphase.[14,19] Such an interphase on the directly charged sample is estimated to be less than 10 nm; however, prelithiation induced much thicker interphases, as indicated by the fact that the shift of these peaks did not occur until etching depth of 40 nm, consistent with the generalization that SEI on anode surface are usually robust and thick, while SEI on cathode are "patch" and often thin.[20] Figure 2d suggests that the SEI formed by prelithiation would not be destroyed by the following charge process, and a good protection sustained in the entire cell life. Both Mn and Co spectra exhibit two simple peaks corresponding to Mn $2p_{3/2}$, Mn $2p_{1/2}$ and Co $2p_{3/2}$, Co $2p_{1/2}$, respectively.[21] No obvious peaks exist on directly charged or prelithiated surfaces, which may be attributed to the low percentage of the two elements in the interphases as shown in the Figure S3b.

Further comparison were made among the samples before and after 100 nm etching, and the spectra of the Li, C, F and O from the sample at different charging/discharging states are shown in Figure S5. No apparent change happens on the pristine sample, but for the charged/prelithiated samples, the proportion of the nonmetallic elements (F, O, and C) decreases and the metallic elements (Ni, Co, and Mn) increases, which confirms the hypothesis that SEI layer is mainly formed by electrolyte and part of the active materials.[19,20]

To examine the difference between the NMC samples that experienced prelithiation at 1.2 V and those that did not, voltage profiles during the first 10 cycles are shown in the


DOI: 10.1021/acs.nanolett.5b02246
Nano Lett. XXXX, XXX, XXX−XXX

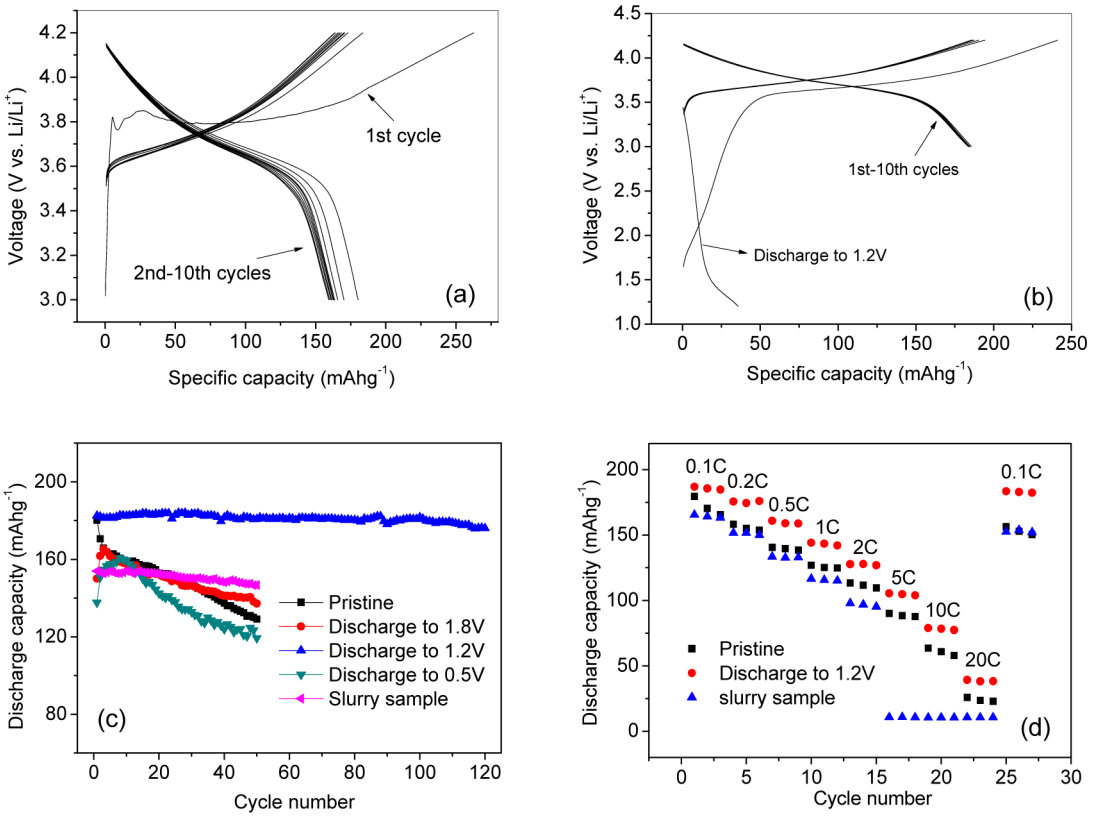


**Figure 3.** Electrochemical performances of various NMC532/CNT composite cathodes: The voltage profiles in the first 10 charge/discharge cycles for the sample without prelithiation (a) and the sample prelithiated to 1.2 V (b), and the cycling stability (c) and rate performances (d) of various samples. All of the tests were operated between 3.0 and 4.2 V using Li as both counter and reference electrodes. For comparison, the cycling and rate performances of the slurry sample were also shown in c and d.

Figure 3a,b. The onset oxidation of the pristine sample starts from 3.8 V in the first cycle, which is much higher than that of the later cycles (about 3.6 V), with a low Coulombic efficiency due to irreversible reactions. Although its initial capacity is as high as computed for the depolarized structure reported previously,[6] it failed to be maintained in subsequent five cyclings, similar to what reported by other groups.[22,23] In sharp contrast, for the NMC532 that experienced prelithiation, the onset oxidation reaction in the very first charge cycle occurs at 3.6 V, which remains constant in all the following cycles. This later feature might suggest that NMC532 cathode may have been structurally transformed by the prelithiation. Although the first charging capacity appears to be excessively large, it is in fact close to the first discharge capacity if the capacity corresponding to prelithiation is subtracted. Thus, the de facto Coulombic efficiency for the initial cycle should be 91.2%, much higher than those without being prelithiated, suggesting that the parasitic reactions between NMC active ingredient and electrolyte must have been effectively suppressed. The SEI formed during prelithiation demonstrated excellent protective nature, as evidenced by the 185 mAh/g capacity, which is close to theoretical value and well-maintained in the extended cyclings as shown in Figure 3c, in strong comparison against the significant capacity fading observed in the first 50 cycles for all other NMC samples that did not experience prelithiation. Although the NMC532 prepared via conventional slurry method shows a good cycling performance, the utilized capacity is much lower than the depolarized NMC samples prepared by filtration method. Compared with the sample made by slurry method, all filtration samples show good rate performance due to the depolarization effect of CNT network as shown in the Figure 3d; naturally, the most conspicuous improvements were achieved in the filtration NMC samples that experienced prelithiation.

In order to reveal the mechanism of how prelithiation affects the capacity and cycling stability of NMC532, cyclic voltammograms (CV) was used to clearly differentiate the corresponding electrochemical processes, as shown in Supporting Information, Figures S6 and S7, and Figure 4. During the first lithiation between 3.0 and 0.5 V, three main peaks appear (Figure S6) at about 1.2, 0.8, and 0.5 V (or lower than 0.5 V), respectively. They are located at about 1.2, 0.8, and 0.5 V (or lower than 0.5 V), respectively. The 1.2 V process is likely related to the reductive reaction of electrolyte and electrode, because its intensity significantly decreases after the first cycle and the potential agrees with what known for SEI formation on anode surfaces. The peak at 0.5 V consistently appears in each cycle with the intensity increasing with the cycle number. According to Figure S6b, it might arise from the collapse of NMC532 lattice and may be responsible for the poor electrochemical performances of the sample predischarged to lower than 1.2 V. The smaller peak that appeared at 0.8 V only in the first prelithiation process may belong to a hitherto unknown electrochemical process of pushing extra Li into NMC lattice. Interestingly, for all NMC532 that subject to direct cycling between 3.0 and 4.2 V, either prepared through slurry or filtration method, an intense oxidation current occurred in the first charging cycle at about 4.2 V on the pristine sample (Figure 4a), then an obvious shift to low voltage happens immediately following the first discharging (Figure 4a), where



DOI: 10.1021/acs.nanolett.5b02246
Nano Lett. XXXX, XXX, XXX−XXX

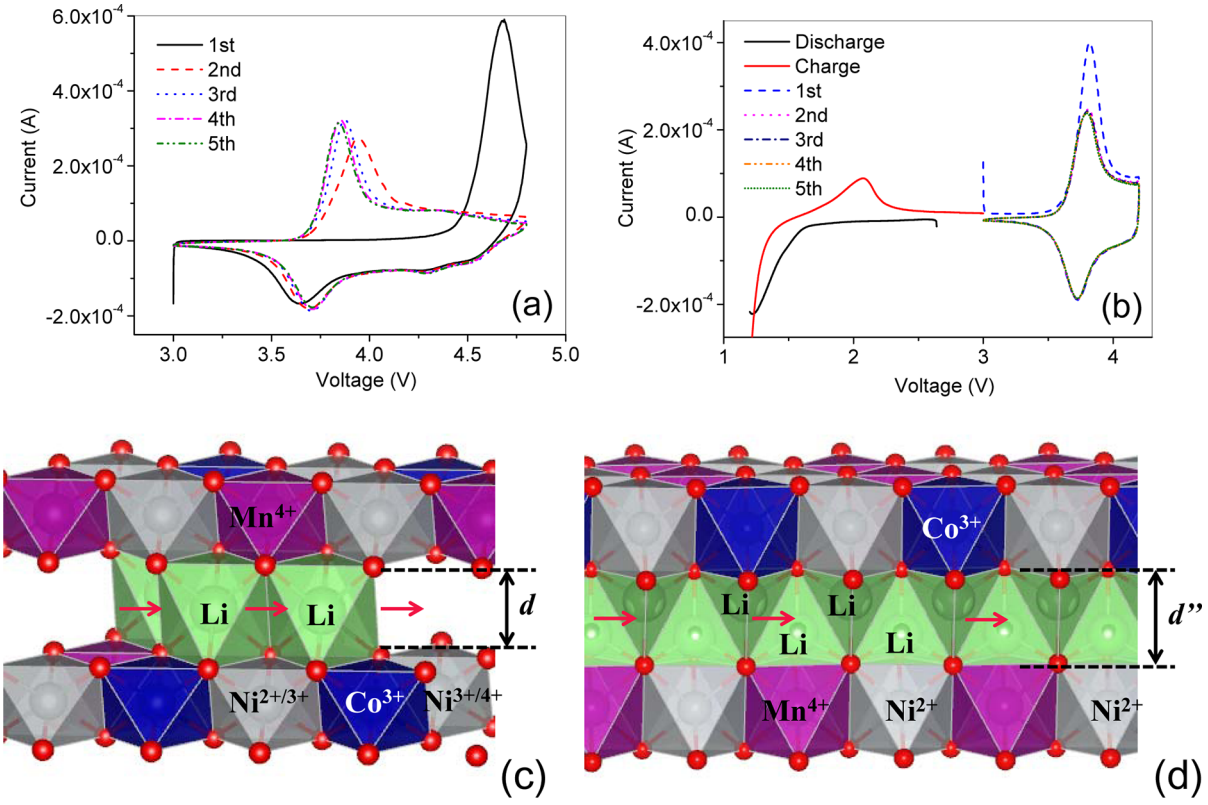


**Figure 4.** Cyclic voltammograms (CV) of various NMC532/CNT composite cathodes: (a) As-prepared sample, (b) sample prelithiated to 1.2 V, (c) schematic structure of NMC532 particle surface without prelithiation, and (d) schematic structure of NMC532 particle surface after prelithiation.

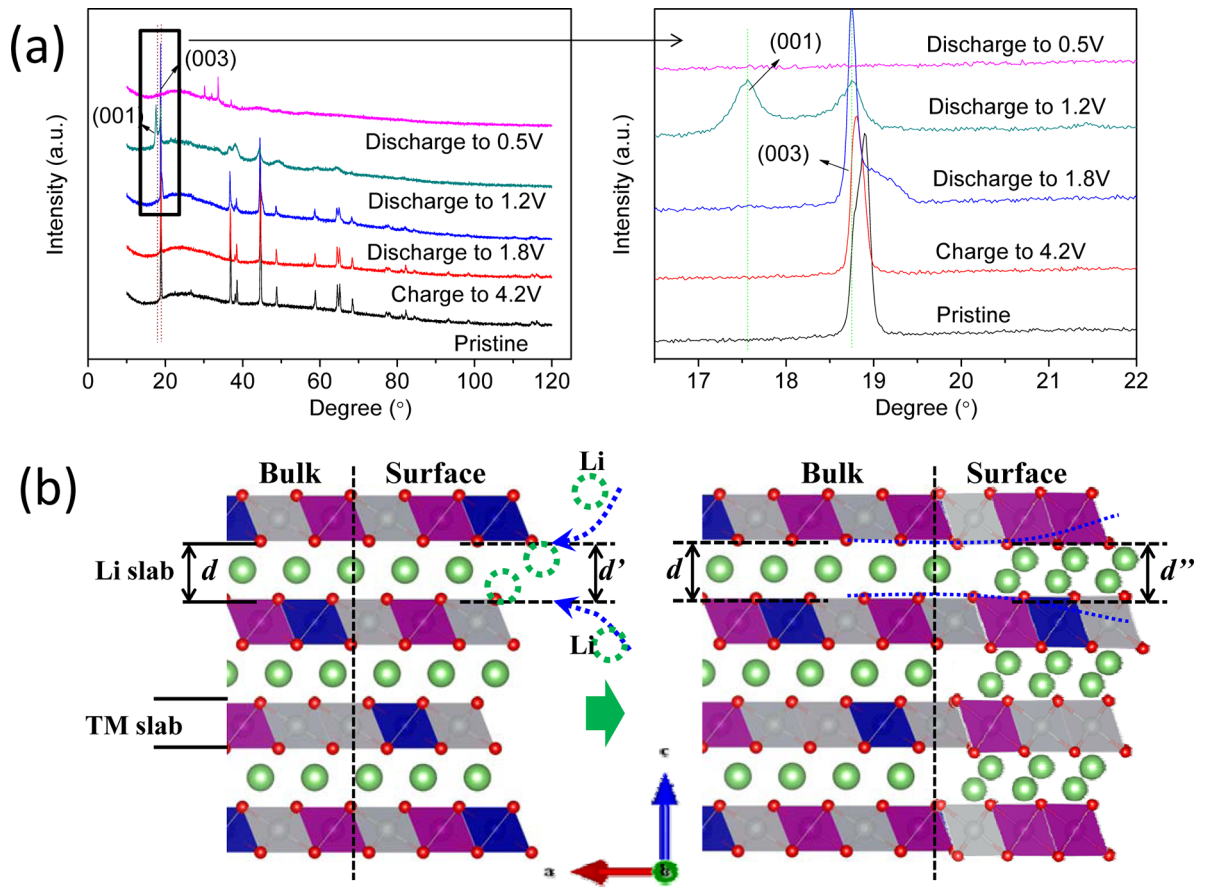


**Figure 5.** XRD of various NMC532/CNT composite cathodes (a) and the schematic mechanisms of its activation in the prelithiation process (b).



DOI: 10.1021/acs.nanolett.5b02246
*Nano Lett.* XXXX, XXX, XXX−XXX

the redox reactions situate at the same potential with the prelithiated NMC532 samples (Figure 4b). The above correlation between the initial oxidation potential and the presence or absence of lithiation may have reflected the structural transformation that was caused by the latter, and we believe that it should be attributed to a process of NMC532 layered structure being lithiated by excess amount of Li (Figure 4c and d).

XRD analysis was conducted on various NMC532/CNT composites that have been prelithiated to varying potentials, and Figure 5a shows the corresponding structure evolutions. Compared with the pristine NMC532, no obvious change was observed in the samples that went through conventional cyclings; however, with the decreasing prelithiation voltage, the NMC features become weaker and wider. When the prelithiation voltage is 1.2 V, a new peak NMC (001) closed to NMC (003) appears, which was also observed in previous work for the layered cathode materials with excess Li that was chemically lithiated.[24] The appearance of this NMC (001) confirms that excessive Li ions are indeed inserted in to the layered lattice of NMC during the prelithiation process and form a double Li layered structure as shown in Figure 5b, perhaps simultaneously with the formation of SEI. Once the prelithiation voltage is lower than 1.2 V (around 0.8 V), the sample shows an amorphous characteristic, which indicates that the NMC532 lattice collapsed because of the excessive insertion of Li.

Using ab initio calculations, here we presented a simplified model for the excessive Li storage in Figure S8, which shows the optimized structures for the normal one layer Li storage scenario ($LiNi_{0.5}Mn_{0.3}Co_{0.2}O_2$) and the excessive two-layer Li storage scenario ($Li_2Ni_{0.5}Mn_{0.3}Co_{0.2}O_2$) between two transition metal slabs. In the former case, the oxygen ions are arranged in a hexagonally close-packed (hcp) array, while the transition metal ions are located at all of the octahedral sites, with the single layer of Li octahedrally coordinated by oxygen. In the latter case, the coordination of transition metal ions and oxygen ions remains unchanged, but the Li ions now are located in all the tetrahedral sites of adjacent layers. Compared with the normal $LiNi_{0.5}Mn_{0.3}Co_{0.2}O_2$, the lattice parameters (a,b,c) of $Li_2Ni_{0.5}Mn_{0.3}Co_{0.2}O_2$ are increased from 14.178 Å, 11.357 Å, and 13.948 Å to 14.76 Å, 11.813 Å, and 15.802 Å, respectively, in which the layer distance along *c*-axis was increased by about 1.9 Å. This is also well consistent with the XRD detection of a new peak NMC (001) close to the (003) peak (Figure 5a) and the corresponding increase of *c*-axis to 1.85 Å according to $\lambda = 2d \sin \theta$. The potential for the excess Li storage was then calculated, and the value of 2.27 V was obtained, according to the following equation:[25]

$$V = -\left\{\frac{E(\mathrm{Li}_{x+\Delta x}R) - E(\mathrm{Li}_{x}R)}{dx} - E(\mathrm{Li})\right\} \quad (1)$$

where $E(\mathrm{Li}_xR)$ and $E(\mathrm{Li}_{x+dx}R)$ stand for the total energy before and after $dx$ lithium ions is removed from Li$R$ compound per formula unit, and $E$(Li) is the total energy of lithium metal. The discharge voltage to insert the excess Li into the layer cathode derived from this calculated potential for the excess Li storage is 1.33 V (3.6 − 2.27 = 1.33 V), very close to the experimental value of 1.2 V.

Regarding the shift of peak potential as shown in the CV during the onset oxidation of the different samples that did not experience prelithiation, there may be two factors responsible: the first one is the protective SEI formed in the prelithiation, which stops the irreversible reactions that induces the shift in the first charging process due to higher impedance, but more likely is the second factor attributed to the valence evolution of Ni. It is well-known that Ni in the NMC532 exists in two valences, $Ni^{2+}$ and $Ni^{3+}$. According to XPS data in Figure 2a, a noticeable shift of the Ni $2p_{3/2}$ peak to lower binding energy was observed with increasing etching depth, which indicates that $Ni^{3+}$ is richer than $Ni^{2+}$ on the surface of NMC532 particles. According to soft X-ray absorption spectroscopy in Figure S9, $Ni^{4+}$ and $Ni^{3+}$ exist on the surface of NMC532 particles. In other words, an inhomogeneous structure of the NMC532 particles could have been made due to the preparation process. In our previous work, we illustrated the two-stage delithiation mechanism in NMC532 materials, the first one being $Ni^{2+}/Ni^{3+}$ located at about 3.8 V, and the other one being $Ni^{3+}/Ni^{4+}$ peaked at 4.0 V or even higher. To the pristine NMC532 particles, $Ni^{3+}$ at the surface will have to experience the first oxidation to $Ni^{4+}$, followed by the $Ni^{2+}/Ni^{3+}$ process deeper in the NMC particle that corresponds to a much larger peak as revealed in the left of Figure 4a. After the first charging and then discharging process, all NMC532 particles will be "unified" to a uniform Ni-valence, and consequently, the onset potential for oxidation reaction drop to 3.8 V and remain constant in the following cycles. For the prelithiated sample, however, all surface $Ni^{4+}$ and $Ni^{3+}$ will be reduced to $Ni^{2+}$ during the lithiation process, while the Li layer is eventually loaded with two slabs of Li-ions. In this situation, the onset oxidation potential for all prelithiated samples would appear at 3.8 V and remain constant thereafter, as shown in the right of Figure 4b. For all the NMC532 samples that subject to direct cycling, there are more $Ni^{3+}$ and $Ni^{4+}$ at and near the sample surface (Figure 4c), the Li-ion diffusion across the surface needs to overcome larger activation barriers,[26] thus leading to an overpotential in the first delithiation process. This overpotential would become smaller and finally vanish after several cycles, because more Li-ions would be inserted at and near the surface to reduce the $Ni^{3+}$ and $Ni^{4+}$ content at and near the sample surface during the lithiation process. By contrast, for the prelithiated NMC532 samples, there are two layers of Li-ion storage at and near the sample surface (Figure 4d), and the voltage for these Li-ion delithiation is lower than that for the normal one layer Li-ion delithiation. This also accounts for the oxidation peak at 2.1 V in the first charge process (Figure 4b), consistent with our following ab initio calculation of 2.27 V. Due to the larger Li slab space at and near the sample surface caused by the excess amount of Li, there is no overpotential for the one layer Li-ions delithiation (Figure 4b).

In conclusion, we propose a prelithiation process to improve both the capacity and cycling stability of NMC532 material. This process brought active material to low voltage before convention charge/discharge cycles, so that a desired solid electrolyte interface (SEI) could be formed. This novel SEI, mainly formed around NMC532/CNT by electrolyte reduction at the thickness of about 40 nm, is chemically similar to SEI found only on anode surfaces without the participation of transition metal and covers the whole surface of NMC532 particles, in sharp contrast to the interphase formed when directly charged to 4.2 V. Two major benefits arose from this novel SEI include the protection of NMC particles from Mn(II)-dissolution and the activation of NMC for extra Li storage. The NMC532/CNT composite cathode thus prepared not only maintains the depolarized structure introduced by


DOI: 10.1021/acs.nanolett.5b02246
Nano Lett. XXXX, XXX, XXX−XXX

filtration method and a high capacity consistent with the theoretic calculation as reported previously, but also excellent cycling performance. This compounded technique of depolarization via nanowiring along with prelithiation can be extended to all cathode materials based on the layered-structure of NMC derivatives, lending us further inspiration to the design and optimization of new composite materials for the next generation lithium batteries.

## ■ ASSOCIATED CONTENT

### Supporting Information

Details of the method section, the morphology, XRD patterns, resistance, electrochemical performances of the prepared samples and the pure CNT samples, the TEMs and soft X-ray data of the interface layer, layered crystal structure simulated by the first principle method. The Supporting Information is available free of charge on the ACS Publications website at DOI: 10.1021/acs.nanolett.5b02246.

## ■ AUTHOR INFORMATION


### Corresponding Author

*Tel./fax: +86-755-26033200. E-mail: panfeng@pkusz.edu.cn (F. Pan).


### Author Contributions

Z.W., S.J., and J.Z. contributed equally.

### Author Contributions

This work was initialized by Z.W., S.J., and F.P. The experiment and electrochemical data was performed by Z.W., S.J., S.X., Q.L., and Z.Z. The data analysis was performed by Z.W., S.J., F.P., Y.L., and W.Y. The calculation was done by Z.H., Y.W., and J. Z. The manuscript was written by Z.W., F.P., K.X., and K.A.

### Notes

The authors declare no competing financial interest.

## ■ ACKNOWLEDGMENTS

This work was financially supported jointly by National Science Foundation of China (No. 51301004), Shenzhen Science and Technology Research Grant (No. JCYJ20140903102215536, CXZZ20120829172325895) and Guangdong - Hong Kong Technology Cooperation Funding (SGLH20120928095706623 and GHP/015/12SZ). Additionally, we acknowledge the support of ShenZhen National SuperComputing Center.

## ■ REFERENCES


(1) Uchaker, E.; Cao, G. *Nano Today* **2014**, *9*, 499−524.
(2) Tarascon, J.-M.; Armand, M. *Nature* **2001**, *414*, 359−367.
(3) Zhan, C.; Lu, J.; Kropf, A. J.; Wu, T.; Jansen, A. N.; Sun, Y. K.; Qiu, X.; Amine, K. *Nat. Commun.* **2013**, *4*, 2437.
(4) Wang, L.; Li, J.; He, X.; Pu, W.; Wan, C.; Jiang, C. *J. Solid State Electrochem.* **2009**, *13*, 1157−1164.
(5) Lin, F.; Markus, I. M.; Nordlund, D.; Weng, T. C.; Asta, M. D.; Xin, H. L.; Doeff, M. M. *Nat. Commun.* **2014**, *5*, 4529.
(6) Wu, Z.; Han, X.; Zheng, J.; Wei, Y.; Qiao, R.; Shen, F.; Dai, J.; Hu, L.; Xu, K.; Lin, Y.; Yang, W.; Pan, F. *Nano Lett.* **2014**, *14*, 4700−4706.
(7) Jung, Y. S.; Cavanagh, A. S.; Riley, L. A.; Kang, S. H.; Dillon, A. C.; Groner, M. D.; George, S. M.; Lee, S. H. *Adv. Mater.* **2010**, *22*, 2172−2176.
(8) Zhang, X.; Belharouak, I.; Li, L.; Lei, Y.; Elam, J. W.; Nie, A.; Chen, X.; Yassar, R. S.; Axelbaum, R. L. *Adv. Energy Mater.* **2013**, *3*, 1299−1307.
(9) Scott, I. D.; Jung, Y. S.; Cavanagh, A. S.; Yan, Y.; Dillon, A. C.; George, S. M.; Lee, S. H. *Nano Lett.* **2010**, *11*, 414−418.
(10) Chen, Z.; Qin, Y.; Amine, K.; Sun, Y. K. *J. Mater. Chem.* **2010**, *20*, 7606−7612.
(11) Lu, J.; Peng, Q.; Wang, W.; Nan, C.; Li, L.; Li, Y. *J. Am. Chem. Soc.* **2013**, *135*, 1649−1652.
(12) Li, X.; Liu, J.; Banis, M. N.; Lushington, A.; Li, R.; Cai, M.; Sun, X. *Energy Environ. Sci.* **2014**, *7*, 768−778.
(13) Kosova, N. V.; Devyatkina, E. T.; Kaichev, V. V. *J. Power Sources* **2007**, *174*, 965−969.
(14) Lee, Y.-M.; Nam, K.-M.; Hwang, E.-H.; Kwon, Y.-G.; Kang, D.-H.; Kim, S.-S.; Song, S.-W. *J. Phys. Chem. C* **2014**, *118*, 10631−10639.
(15) Amine, K.; Tukamoto, H.; Yasuda, H.; Fujita, Y. *J. Electrochem. Soc.* **1996**, *27*, 1607−1613.
(16) Mahata, N.; Cunha, A. F.; Orfao, J. J. M.; Figueiredo, J. L. *Appl. Catal., A* **2008**, *351*, 204−209.
(17) Hoffer, B. W.; Crezee, E.; Devred, F.; Mooijman, P. R. M.; Sloof, W. G.; Kooyman, P. J.; Langeveld, A. D.; Kapteijn, F.; Moulijn, J. A. *Appl. Catal., A* **2003**, *253*, 437−452.
(18) Rodella, C. B.; Kellermann, G.; Francisco, M. S. P.; Jordao, M. H.; Zanchet, D. *Ind. Eng. Chem. Res.* **2008**, *47*, 8612−8618.
(19) Edström, K.; Gustafsson, T.; Thomas, J. O. *Electrochim. Acta* **2004**, *50*, 397−403.
(20) Xu, K. *Chem. Rev.* **2014**, *114*, 11503−11618.
(21) Myung, S.-T.; Izumi, K.; Komaba, S.; Sun, Y.-K.; Yashiro, H.; Kumagai, N. *Chem. Mater.* **2005**, *17*, 3695−3704.
(22) Ban, C.; Li, Z.; Wu, Z.; Kirkham, M. J.; Chen, L.; Jung, Y. S.; Payzant, E. A.; Yan, Y.; Whittingham, M. S.; Dillon, A. C. *Adv. Energy Mater.* **2011**, *1*, 58−62.
(23) Luo, S.; Wang, K.; Wang, J.; Jiang, K.; Li, Q.; Fan, S. *Adv. Mater.* **2012**, *24*, 2294−2298.
(24) Johnson, C. S.; Kim, J.-S.; Kropf, A. J.; Kahaian, A. J.; Vaughey, J. T.; Fransson, L. M. L.; Edstrom, K.; Thackeray, M. M. *Chem. Mater.* **2003**, *15*, 2313−2322.
(25) Ceder, G.; Ven, A. V.; Marianetti, C.; Morgan, D. *Modell. Simul. Mater. Sci. Eng.* **2000**, *8*, 311−321.
(26) Kang, K.; Ceder, G.; Grey, C. P.; Breger, J.; Meng, Y. S. *Science.* **2006**, *311*, 977−980.




DOI: 10.1021/acs.nanolett.5b02246
*Nano Lett.* XXXX, XXX, XXX−XXX